

# Radiological, vascular osteochondrosis occurs in the distal tarsus, and may cause osteoarthritis

Sigurdur F. Sigurdsson<sup>1</sup> | Kristin Olstad<sup>1</sup>  | Charles J. Ley<sup>2</sup> | Sigríður Björnsdóttir<sup>3</sup>  | David J. Griffiths<sup>4</sup> | Cathrine T. Fjordbakk<sup>1</sup>

<sup>1</sup>Faculty of Veterinary Medicine, Department of Companion Animal Clinical Sciences, Equine Section, Norwegian University of Life Sciences, Oslo, Norway

<sup>2</sup>Department of Clinical Sciences, Swedish University of Agricultural Sciences, Uppsala, Sweden

<sup>3</sup>Agricultural University of Iceland, Hvanneyri, Iceland

<sup>4</sup>Faculty of Veterinary Medicine, Department of Basic Sciences and Aquatic Medicine, Anatomy Section, Norwegian University of Life Sciences, Oslo, Norway

## Correspondence

Kristin Olstad, Norwegian University of Life Sciences, Faculty of Veterinary Medicine, Department of Companion Animal Clinical Sciences, Equine Section, Ullevålsveien 72, 0454 Oslo, Norway.  
Email: kristin.olstad@nmbu.no

## Funding information

This study was funded by grant number H-16-47-192/NFR272326 from the Swedish-Norwegian Foundation for Equine Research/Research Council of Norway, with contributions from Norsk hestesenter and Jordbruksavtalen.

## Abstract

**Background:** Osteochondrosis occurs due to failure of the blood supply to growth cartilage. Osteochondrosis lesions have been identified in small tarsal bones and suggested to cause distal tarsal osteoarthritis; however, it has not been determined whether distal tarsal osteochondrosis lesions were the result of vascular failure.

**Objectives:** To perform post-mortem arterial perfusion and micro-computed tomography (CT) of the central (CTB) and third tarsal bones (TIII) of fetuses and foals up to 5 months old, to describe tarsal development and any lesions detected.

**Study design:** Descriptive, nonconsecutive case series.

**Methods:** Twenty-three animals that died or were euthanased from 228 days of gestation to 5 months old were collected, comprising two fetuses and nine foals of miscellaneous breeds and 12 Icelandic Horse foals, a breed with high prevalence of distal tarsal osteoarthritis. One hindlimb from each foal was perfused arterially with barium, and the CTB and TIII were examined with micro-CT.

**Results:** Perfusion yielded partial information from 41% of the animals. The CTB and TIII were supplied by nutrient arteries and perichondrial vessels with vertical, transverse and circumferential configurations. Fourteen of the 23 (61%) animals had focal defects in the ossification front, that is, radiological osteochondrosis. The majority of lesions matched the configuration and development of vertical vessels. Additionally, full-thickness, cylindrical defects matched transverse vessels, and the long axes of some dorsal lesions matched circumferential vessels.

**Main limitations:** Lack of histological validation.

**Conclusions:** Post-mortem perfusion was poor for examination of the blood supply to the growth cartilage of the CTB and TIII. Radiological osteochondrosis lesions were compatible with vascular failure because they were focal, and because lesion geometry matched vessel configuration. The relationship between osteochondrosis and distal tarsal osteoarthritis warrants further investigation.

The work was conducted at the Norwegian University of Life Sciences, Oslo, Norway.

The abstract is available in Portuguese in the Supporting Information section of the online version of this article

This is an open access article under the terms of the Creative Commons Attribution-NonCommercial-NoDerivs License, which permits use and distribution in any medium, provided the original work is properly cited, the use is non-commercial and no modifications or adaptations are made.

© 2021 The Authors. *Equine Veterinary Journal* published by John Wiley & Sons Ltd on behalf of EVJ Ltd.

**KEYWORDS**

horse, cartilage canal blood supply, distal tarsal osteoarthritis, foal, growth cartilage, osteochondrosis, vascular failure

## 1 | INTRODUCTION

The developmental orthopaedic diseases are common in young horses.<sup>1</sup> Some may be a result of osteochondrosis,<sup>1</sup> which is defined as a disturbance in endochondral ossification.<sup>2</sup> Failure of the temporary, end-arterial blood supply leads to ischaemic chondronecrosis at intermediate depth of growth cartilage.<sup>3-5</sup> When the ossification front advances to surround an area of chondronecrosis, it causes a focal delay in endochondral ossification.<sup>3-5</sup> Osteochondrosis can resolve,<sup>6,7</sup> or progress to osteochondrosis dissecans or subchondral bone cysts.<sup>2,5,8</sup> Cuboidal bones are affected by slightly different developmental diseases than long bones.<sup>1</sup> Incomplete ossification<sup>9</sup> and wedging<sup>10</sup> occur in foals, whereas distal tarsal osteoarthritis (synonyms: bone spavin and<sup>11</sup> juvenile arthritis<sup>1</sup>) occur in slightly older horses. Some breeds like the Icelandic Horse are heritably predisposed<sup>12</sup> and have high prevalence<sup>13</sup> of distal tarsal osteoarthritis. With histological examination, osteochondrosis lesions were documented in distal tarsal bones and it was suggested that they could lead to osteoarthritis.<sup>11</sup> It was not determined whether distal tarsal osteochondrosis was a result of failure of the blood supply to growth cartilage.<sup>11</sup> The blood supply to distal tarsal bones has been studied, but only in  $\geq 6$ -month-old horses.<sup>14</sup> The blood supply to growth cartilage regresses from distal limb joints at a younger age than from proximal limb joints,<sup>3,4,15,16</sup> and it regressed from the tarsocrural joint, the examined joint that is nearest to the distal tarsal joints, at 7-10 weeks of age.<sup>3,4</sup> To study the blood supply to growth cartilage, it is therefore necessary to examine the central (CTB) and third (TIII) tarsal bones of foals younger than 6 months old.

Arterial contrast-enhanced micro-computed tomography (CT) was previously used to study blood supply and osteochondrosis in the tarsocrural joint of foals.<sup>17</sup> With contrast-enhanced micro-CT, it is possible to identify focal vascular failure if there are sufficient remaining adjacent, patent vessels to outline it.<sup>17</sup> Computed tomography is uniquely suited for imaging bone, and in skeletally immature animals, the bone contour represents the junction between growth cartilage and subchondral bone, that is, the ossification front.<sup>17</sup> Computed tomography is therefore also highly suited for detecting osteochondrosis lesions from the stage that they cause a delay in endochondral ossification.<sup>17,18</sup> Originally, arterial contrast perfusion was carried out as a terminal procedure,<sup>4</sup> but others have reported successful post-mortem perfusion.<sup>14,19-21</sup> The aim of this study was to perform post-mortem arterial perfusion and micro-CT of the CTB and TIII of fetuses and foals up to 5 months old, to describe development and any lesions detected, including osteochondrosis because it is a suggested cause of distal tarsal osteoarthritis.

## 2 | MATERIALS AND METHODS

The animals originated from stud farms in Iceland, and from the teaching hospital of the Norwegian University of Life Sciences. The material consisted of aborted fetuses and foals of any breed and sex. Fetal age was determined by the date of the last covering as reported by the mare owner. The upper age limit for inclusion was 5 months. All available clinical records were gathered, including cause of death or euthanasia. As soon as possible after death, one hindlimb (preferably the left) was harvested by disarticulating the stifle, or by sawing across the tibia. Most limbs were frozen, and limbs collected in Iceland were transported to Norway on dry ice.

### 2.1 | Arterial perfusion

All limbs were thawed and weighed before perfusion according to the procedures described in Hertsch and Samy<sup>21</sup> and Olstad et al.<sup>4</sup> Briefly, limbs were catheterised in the femoral or cranial tibial artery and flushed with normal saline, then perfused with a 20% v/vol solution of barium in normal saline, followed by a 20% v/vol solution of barium in 4% phosphate-buffered formalin. The skin was removed, and the tarsus was collected and fixed in 4% phosphate-buffered formalin for 48 hours, before being transferred to 75% ethanol.

### 2.2 | Measurements and sample blocks

The talus was removed, and the maximal mediolateral width, dorso-plantar depth and proximodistal height of the CTB were measured. The CTB was hand-sawed into approximate medial and lateral halves (Figure S1A). The CTB was separated from the TIII by sharp dissection, starting at the saw-cut dorsally and continuing around the periphery while taking care to preserve the perichondrium. The TIII was measured, sawed and dissected in the same way as the CTB (Figure S1B), resulting in four sample blocks for micro-CT scanning per limb.

### 2.3 | Micro-CT

The sample blocks were wrapped in sealing film (Parafilm<sup>®</sup>; Merck) and scanned using a multi-scale nano-tomograph with an open-type x-ray tube (Skyscan 2211; Bruker Corporation). A 0.5 mm titanium filter was used to remove low-energy x-rays from the beam. The samples were mounted on a stage using modelling clay and rotated at steps of 0.43° per projection. The images were acquired using a

flat-panel detector, at 80 kV, 55  $\mu$ A and an exposure time of 280 ms, with an isotropic voxel size of 25  $\mu$ m. Images were reconstructed using the manufacturer's software (NRecon; Bruker Corporation), and viewed using commercial software (VGStudio Max, version 3.2.4; Volume Graphics).

## 2.4 | Skeletal maturity and normal development

Included animals had an owner-reported age, and some animals had an owner-reported or clinical diagnosis of being premature. Reading of the micro-CT scans therefore started with an evaluation and relative ranking of skeletal maturity.

All scans were read by S.F.S., K.O. and C.T.F. with >60 years' post-graduate experience and >17 years' experience with micro-CT. Each scan was viewed in three orthogonal planes and as 3D models. Seven standardised views were printed and used to rank scans relative to each other: proximal, distal, dorsal, plantar, axial and abaxial views of the bone isosurface model, and a proximal view of the barium isosurface model, referred to as the vascular view. Skeletal maturity was evaluated by registering the presence of the ossification centre, presence of dimples in the ossification front previously documented at points where arterioles course from bone into growth cartilage in young foals,<sup>17</sup> sharpness of the inter-tarsal ligament fossa margins (Figure S1) and presence of the plantar-medial tubercle of the CTB (Figure S1A) and the dorsomedial ridge of the TIII (Figure S1B).<sup>22</sup> For skeletal maturity, all readers discussed until a consensus ranking was reached, which was then used to describe development.

## 2.5 | Perfusion quality

The technical quality of the arterial perfusion was assessed by identifying the most complete perfusion and ranking all other perfusions relative to it. Perfusion quality was evaluated by assessing evenness of distribution, branching and consistent tapering of barium contrast column termini to a point systematically in the perichondrium, subchondral bone and growth cartilage. The readers used the printed vascular views and discussed until consensus was reached.

## 2.6 | Blood supply

Blood supply was described in terms of vessel entry points into the CTB and TIII, approximate course and branching. Branching was divided into a monopodial pattern, characterised by few branches far apart, and dichotomous branching, characterised by a high number of branches close together from a few points.<sup>23</sup> Foci of intense dichotomous branching within subchondral bone were referred to as sinusoids.<sup>19</sup>

## 2.7 | Radiological osteochondrosis and other lesions

The ossification front is normally irregular during growth. Based on previous histologically validated micro-CT<sup>17</sup> and conventional CT studies,<sup>18</sup> any changes that were peripheral, gradual and diffuse were interpreted as representative of normal growth irregularity.

The interpretation of changes as representative of osteochondrosis lesions was based on previous histologically validated micro-CT and conventional CT studies.<sup>17,18</sup> Radiological osteochondrosis lesions were defined as focal, sharply demarcated, uniformly hypodense defects located in or near the ossification front.<sup>17,18</sup> In order to be counted as lesions, defects had to be present in  $\geq 2$  consecutive slices of  $\geq 2$  orthogonal planes. All defects or changes close together in the ossification front towards one aspect of a bone were counted as a single lesion, meaning one lesion could have  $\geq 1$  hypodense defect. Defects that were spherical and surrounded by relatively more bone than osteochondrosis lesions were referred to as cysts.<sup>8</sup> Changes that have been documented to represent secondary responses, mainly mineralised bodies representing reparative ossification centres adjacent to lesions,<sup>5,17</sup> were registered. For the absence or presence of lesions, all readers agreed on every occasion, that is, there was no dissent.

## 3 | RESULTS

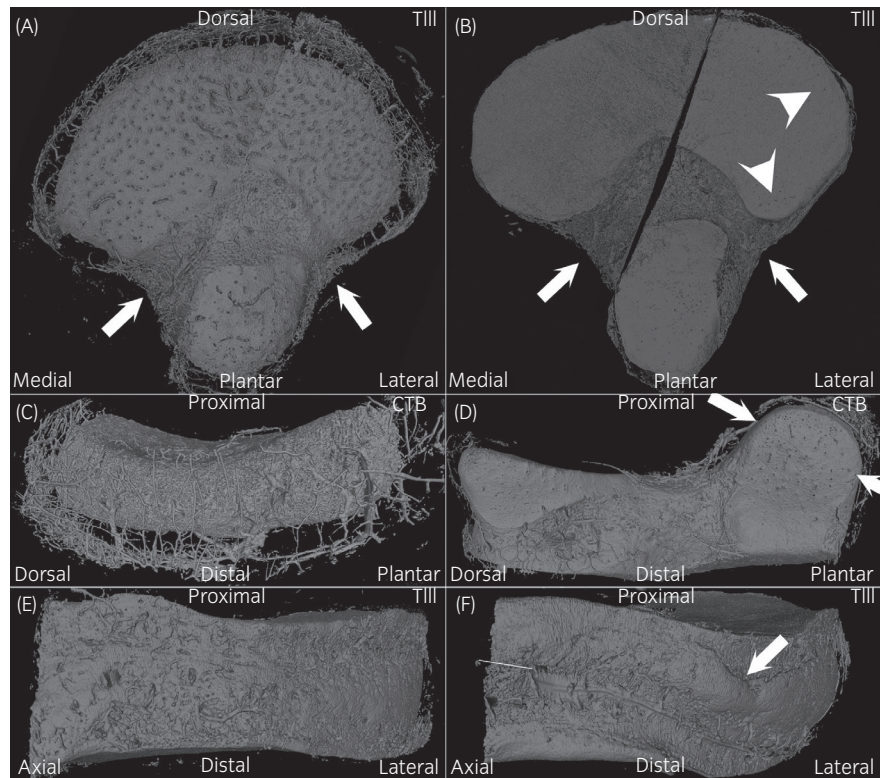
The population consisted of two fetuses and 21 foals: animals 1-12 were Icelandic Horse foals from 0-150 days old, and animals 12-23 were fetuses and foals of miscellaneous breeds from 228 days of gestation to 122 days old. Available characteristics are summarised in Table S1, including that in the breed-matched Icelandic group, height increased by 4 and 5 mm from the smallest to the largest TIII and CTB, respectively, whereas width and depth increased by 15-18 mm, that is,  $\geq 3$  times as much.

### 3.1 | Skeletal maturity and normal development

The evaluation of skeletal maturity is summarised in Table S2. Fetuses 13 (228 days of gestation) and 14 (270 days of gestation) had no ossification centres, compatible with their gestational age. Foals 3 and 15 were not considered to represent normal development, described in Section 3.5 Other lesions below. All remaining 19 foals had ossification that was consistent with their reported age, and were used to describe development.

Dimples were uniformly present over the entire surface of the ossification centre in young foals (Figure 1A), present only peripherally at intermediate age (Figure 1B) and absent in old foals. There was some variability in the presence of dimples between surfaces, bones, animals and groups, detailed in Table S2. The last surface with peripheral dimples was the proximal surface of TIII in foal 22 (58 days). Dimples were not seen in the ossification front of any foal  $\geq 105$  days old.

**FIGURE 1** Normal development. A, At 7 d, dimples are uniformly present over the entire proximal surface of the ossification centre in the third tarsal bone (TIII), and the margins of the ligament fossae (arrows) are softly rounded. B, At 46 d, dimples are only present peripherally (arrowheads), and the ligament fossa (arrows) margins are sharp. C, At 7 d, the plantaro-medial tubercle of the central tarsal bone (CTB) is absent, and D, at 46 d, the plantaro-medial tubercle (between arrows) is present. E, At 46 days, the dorsomedial ridge of TIII is absent, and F, at 58 days, the dorsomedial ridge is present. A, C, Foal 17. B, D, E, Foal 21, F, Foal 22. A-B, Proximal views; C-D, Medial views; E-F, Dorsal views of 3D isosurface models of bone and barium



The margins of the inter-tarsal ligament fossae were softly rounded in the youngest foals (Figure 1A), a mixture of soft and sharp at intermediate age, and sharp in the oldest foals (Figure 1B). Notably, the number of ligament fossae varied between animals, independent of maturity (Table S2). The plantar-medial tubercle of the CTB was consistently present in all foals  $\geq 42$  days (Figure 1C,D), and the dorsomedial ridge of TIII was present in all foals  $\geq 58$  days (Figure 1E,F).

### 3.2 | Perfusion quality and systematic description of the blood supply

The evaluation of perfusion quality is presented in Table S3, except fetus 13 that was not evaluated due to lack of hyperdense landmarks. The perfusion in foal 21 was the most complete (Figure 2A). The remaining perfusions comprised eight partial perfusions that yielded some useful information, and 13 incomplete perfusions that yielded no useful information, thus perfusion yielded partial information from 9/22 (41%) animals. In light of this discovery, generating a systematic description of the blood supply was abandoned. Sinusoids were described, due to an interest in the suitability of micro-CT for this purpose. It was readily possible to distinguish between evenly perfused bone (Figure 2A) and sinusoids (Figure 2B,C). Eighteen of the 22 animals had  $\geq 1$  sinusoid in  $\geq 1$  bone (Table S3). Small-to-large sinusoids consisted of narrow barium columns that were regular and well-organised (Figure 2B). Extra-large sinusoids consisted of barium columns and large, coalescing barium spheres (Figure 2C). Images of a partial perfusion,

under- and overfilling of different tissues with barium are available in Figure S2.

### 3.3 | Opportunistic description of the blood supply

The nine animals with partial perfusions were used to describe the visible portion of the blood supply. The CTB and TIII were supplied by a central system of nutrient arteries, and a peripheral system of perichondrial arteries. The nutrient arteries approached the CTB and TIII via the inter-tarsal ligament fossae as detailed in Table S2, and followed a diverging course from the centre towards the periphery. The largest diameter, central trunks tended to bi-/trifurcate, whereas smaller diameter vessels towards the periphery branched more frequently, including dichotomous branching and sinusoids.

Perichondrium was only present on the abaxial surface around the periphery of the CTB and TIII. Perichondrial vessels entered growth cartilage at regular intervals around the periphery (Figure 2A), including that some vessels entered where the dorsal tarsal ligament inserted. Most vessels entered at a level that corresponded to mid-height of the ossification centre, but vessels also entered at a level that was near the proximal or distal ossification front (Figure 3A). Perichondrial vessels initially followed a converging course from the abaxial periphery towards the ossification centre (Figure 2A). However, after a distance, it was common for the vessel trunk itself or branches of it to make a 90° turn and continue in the proximal or distal direction towards one ossification front, that is, vertically (Figure 3B). Vessels entering at mid-height of the ossification centre then ended up coursing vertically for part of the height of

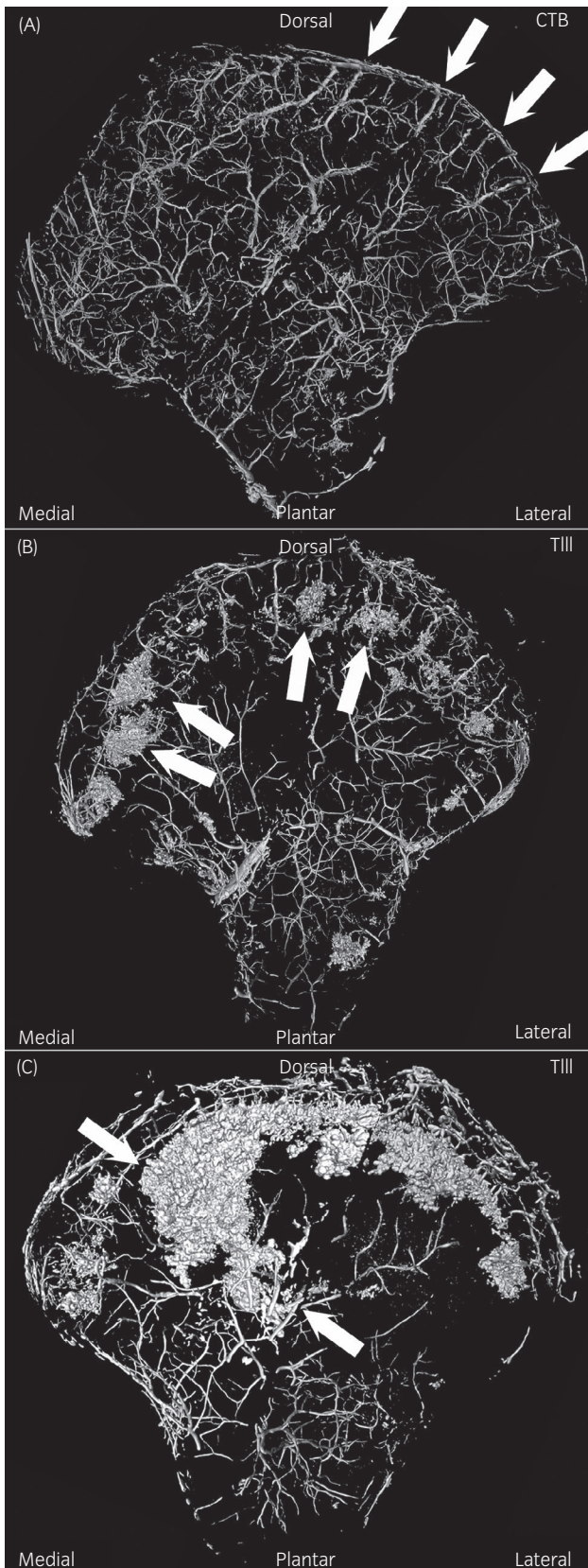


**FIGURE 2** Perfusion quality and sinusoids. A, The perfusion of the central tarsal bone (CTB) of foal 21, judged to be the most complete. Vessels enter the growth cartilage at regular intervals (arrows) around the periphery. B, Multiple, small-to-medium foci of intensely dichotomously branching vessels (arrows) referred to as sinusoids are readily appreciable within the otherwise evenly perfused third tarsal bone (TIII) of foal 17. C, An untidy and irregular, extra-large sinusoid (between arrows) that includes large, coalescing barium spheres is visible in the TIII of foal 6. All images are proximal views of 3D isosurface models of barium

of the mid-portion of partial and full-height vertical vessels being surrounded by and incorporated into bone, while the proximal and/or distal portions remained in growth cartilage (Figure 3D). Such vessels sometimes gave off small side branches (Figure 3D). Mid-way between the periphery and centre, there were examples of vessels that appeared to be of perichondrial-arterial origin, but where the ossification front had surrounded most of the trunk of the vessel and only the very proximal and distal tips protruded into growth cartilage (Figure 3E). Such vessels traversed the entire thickness of the ossification centre, and were therefore referred to as transverse vessels. Near the centre, there were also some transverse vessels of nutrient-arterial origin (Figure 3E).

Instead of turning proximally or distally, a few perichondrial vessels made a 90° turn in the medial or lateral direction and continued in the horizontal plane, roughly parallel with the circumference of the ossification centre (Figure 3F). Circumferential vessels were mainly observed at the dorsomedial or dorsolateral corners of the CTB and TIII, where they were located either at mid-height, or near the proximal or distal front of the ossification centre.

### 3.4 | Osteochondrosis lesions

Fourteen of the 23 (61%) animals had changes that fitted our definition of osteochondrosis lesions distributed as 9/12 (75%) Icelandic foals and 5/9 (55%) foals of miscellaneous breeds. Neither fetus ( $n = 2$ ) had osteochondrosis lesions. The 14 animals had 24 lesions, all consisting of variable number, size and shape focal defects in the ossification front, identified by lower-case letters from *a* to *x* and foal number as listed in Table 1.

Twelve lesions, *a2-l22* (Figure 4A,B), were located at or near margins in regions that corresponded to where the distal tips of vertical vessels traversed the ossification front after incorporation of vessel mid-portions into bone (Figure 3D). Because they were collected from actively growing foals, shallow defects near the periphery, like lesions *a2-h8*, were interpreted as lesions of short duration (Figure 4A), whereas deeper defects located near the axial centre, like lesions *i20-l22*, were interpreted as lesions of long duration (Figure 4B). The defects in lesions *i20-l22* were deep, hemi-spherical and fitted the definition of cysts.

The three lesions *m22-o12* were located at mid-height of a peripherally abaxial ossification front, whereas the three lesions *p11-r6* comprised multiple defects, located both at mid-height and near

the ossification centre (Figure 3B), whereas vessels entering growth cartilage near the proximal or distal ossification front coursed vertically for the entire height of the ossification centre (Figure 3C). Near the periphery of the CTB and TIII, there were frequent examples

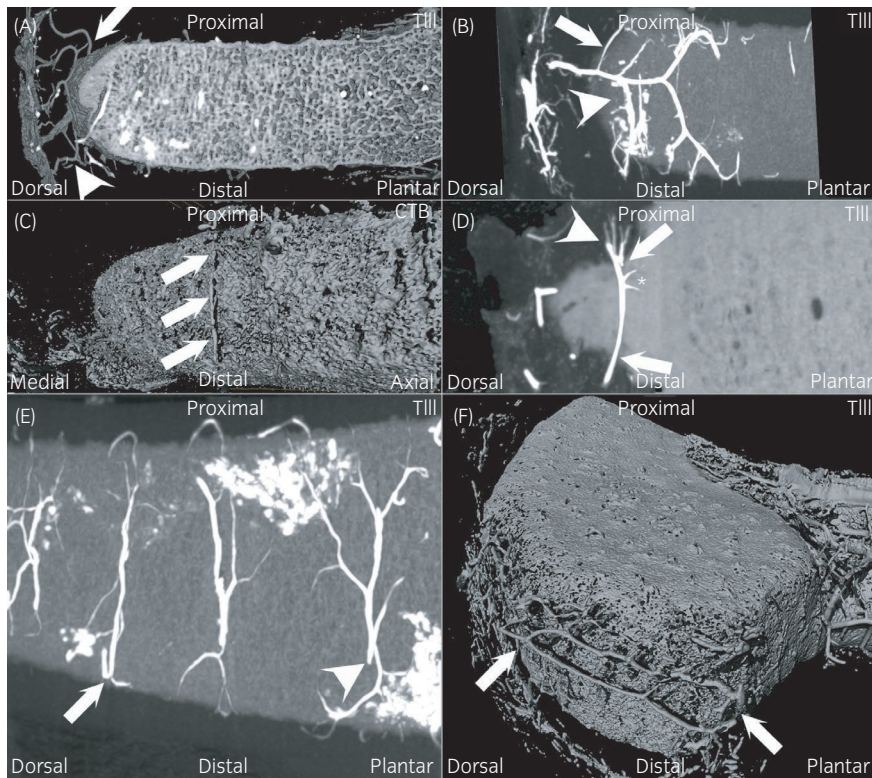


**FIGURE 3** Vertical, transverse and circumferential vessels. A, Perichondrial arteries enter the growth cartilage at different height levels of near the proximal front (arrow), near the distal front (arrowhead) or at mid-height of the ossification centre of the third tarsal bone (TIII) of foal 17. B, A perichondrial vessel gives off branches that make 90° turns in the proximal (arrow) and distal (arrowhead) directions and continue vertically for part of the ossification centre in foal 17. C, A perichondrial vessel (arrows) courses vertically for the entire height of the ossification centre in the central tarsal bone (CTB) of foal 1. D, The mid-portion of a vertical vessel is incorporated into bone (between arrows) while the proximal (arrowhead) and distal portions remain located within the growth cartilage of foal 12. The trunk gives off two small side branches (asterisk). E, Transverse vessels traverse the entire thickness of the ossification centre in foal 17. Nearest the periphery, transverse vessels (arrow) appeared to be of perichondrial-arterial origin, whereas near the centre, transverse vessels (arrowhead) appeared to be of nutrient-arterial origin. F, A perichondrial vessel (between arrows) makes a 90° turn and continues parallel with the circumference of the ossification centre in foal 5. A-B, D-E, Sagittal slices, C, Dorsal view and F, Medial view of 3D bone and barium isosurface models

margins where vessels traversed the ossification front after incorporation (Figure 4C,D). Lesions *q15* (Figure 4C) and *r6* (Figure 4D; Video S1) each included two defect lobes that were roughly aligned in the proximodistal direction, matching the configuration of vertical vessels with side branches (Figure 3D). Superficially adjacent to lesion *r6*, there was an intact, vertical vessel with two side branches where one branch was surrounded by a mineral density with trabecular structure, interpreted as a separate centre of reparative ossification in response to lesion *r6* (Figure 4D; Video S1).

The two lesions *s16* and *t16* consisted of two and three vertical, full-thickness cylindrical defects in the CTB and TIII respectively (Figure 4E,F). Cylindrical defects matched the configuration of transverse vessels (Figure 3E), including smaller side defects matching side branches (Figure 4F). Lesions *s16* and *t16* were located mid-way between the periphery and centre, interpreted as long duration.

The long axes of the three defects in lesion *u2* dorsomedially (Figure 5A) and lesions *w22-x22* dorsolaterally (Figure 5B,C; Video S2) were parallel with circumferential vessels (Figure 3F). The shallow, ovoid defect in lesion *u2* was located peripherally and considered

to be of short duration (Figure 5A), whereas the deep, groove defect in lesion *x22* was located mid-way between the periphery and centre and interpreted as long duration (Figure 5C). The final change referred to as lesion *v2* consisted of a large vessel surrounded by a mineral tube with trabecular structure (Figure 5D), protruding from the distal CTB ossification front directly opposite, and interpreted as a reparative response to lesion *u2* in TIII (Figure 5A).

### 3.5 | Other lesions

Foal 1 had multiple shallow, patch-like areas in both the CTB and TIII with thinner trabeculae and larger intervening, hypodense spaces, that is, where the ossification front appeared coarser than the rest (Figure S3A-B), but where the spaces were not as large as the osteochondrosis defects described above. The ossification of foals 3 and 15 was inconsistent with their reported age (Figure S3C-F). The CTB of foal 3 (1 day) consisted only of cartilage, whereas the TIII of foal 3 and the CTB of foal 15 (2 days)

**TABLE 1** Lesions identified with micro-CT in the distal tarsus of a population aged from 228 d of gestation to 5 mo

Lesion	Animal	Observation	Height-wise location	Abaxio-axial location	Aspect	Half	Bone	Secondary response	Comment
<i>a</i>	2	1x very small, shallow ovoid defect	Proximal margin of TII/II facet	Peripheral	Plantar	Medial	TIII	None	Also small, smooth, drop-shaped defect in dorsal midline of proximal CTB ossification front
<i>b</i>	10	1x very small, shallow, ovoid defect	Proximal margin of tubercle	Peripheral	Plantar	Lateral	CTB	None	None
<i>c</i>	7 <sup>a</sup>	1x very small, shallow, ovoid defect	Proximal margin of TIV facet	Peripheral	Plantar	Lateral	TIII	None	Subchondral bone: heterogeneous structure with diffuse, hypodense foci without trabeculae
<i>d</i>	10	1x small, shallow, multi-lobulated defect	Proximal margin of ridge	Peripheral	Dorsomedial	Medial	TIII	None	Near dorsal tarsal ligament
<i>e</i>	9	1x small, shallow, multi-lobulated defect	Towards plantar margin of TIII facet	Peripheral	Distal	Medial	CTB	None	None
<i>f</i>	23 <sup>a</sup>	1x small, shallow, triangular defect	Proximal margin of tubercle	Peripheral	Plantar	Medial	CTB	None	None
<i>g</i>	4	1x small, shallow, bi-lobed defect	Proximal margin of tubercle	Peripheral	Plantar	Medial	CTB	None	None
<i>h</i>	8	2x medium, shallow, ovoid defects: one relatively plantaro-axial and the other relatively medio-abaxial	Proximal margin of tubercle	Peripheral	Plantar	Medial	CTB	None	Subchondral bone: heterogeneous with sharp, circular hypodense foci and regions with larger marrow spaces and fewer, thinner trabeculae
<i>i</i>	20 <sup>a</sup>	1x medium, hemi-spherical cyst	Distal ossification front of CTB	Mid-way	Distal	Medial	CTB	None	Small, hypodense lollipop-shaped defect in dorsal midline of proximal CTB ossification front
<i>j</i>	20 <sup>a</sup>	2x medium to small, hemi-spherical cysts: one relatively abaxial, the other relatively axial	Proximal ossification front of TIII	Mid-way	Proximal	Medial	TIII	None	Defect <i>j</i> is deeper than defect <i>i</i>
<i>k</i>	22 <sup>a</sup>	1x medium, hemi-spherical cyst	Distal ossification front of CTB	Mid-way	Distal	Medial	CTB	None	None
<i>l</i>	22 <sup>a</sup>	1x large, hemi-spherical cyst	Proximal ossification front of TIII	Mid-way	Proximal	Medial	TIII	None	Defect <i>l</i> is deeper than defect <i>k</i>
<i>m</i>	22 <sup>a</sup>	1x small, shallow, multi-lobulated defect	Mid-height of tubercle	Peripheral	Plantar	Medial	CTB	None	None
<i>n</i>	10	1x small, shallow, ovoid defect	Mid-height of CTB ossification front	Peripheral	Abaxial	Medial	CTB	None	None

(Continues)

TABLE 1 (Continued)

Lesion	Animal	Observation	Height-wise location	Abaxio-axial location	Aspect	Half	Bone	Secondary response	Comment
<i>o</i>	12 <sup>a</sup>	1x medium, shallow, multi-lobulated defect	Mid-height of tubercle	Peripheral	Plantar	Medial	CTB	None	None
<i>p</i>	11	2x medium, shallow, multi-lobulated defects: one at mid-height and one near proximo-axial margin	Mid-height and proximo-axial margin of tubercle	Peripheral	Plantar	Medial	CTB	None	None
<i>q</i>	15	3x deep defects: one small, triangular dorsal defect, one medium lateral defect and one large, multi-lobulated plantar defect	Mid-height and towards proximal margin	Peripheral	Dorsal, lateral, plantar	Lateral	TIII	None	Less ossified than age-matched comparison; potential incomplete ossification (see text)
<i>r</i>	6 <sup>a</sup>	1x small, shallow, bi-/multi-lobulated defect	Mid-height and towards proximal margin of tubercle	Peripheral	Plantar	Lateral	CTB	Vascular proliferation, ossification centre	Also conical, hypodense, cyst-like area around nutrient foramen distal TIII
<i>s</i>	16 <sup>a</sup>	2x defects: one medial and one lateral large, full-thickness cylindrical defect	Entire height of ossification centre	Mid-way	Proximal and distal	Medial and lateral	CTB	Adjacent ossification impinges	None
<i>t</i>	16 <sup>a</sup>	3x defects: one medial, one middle and one lateral large, full-thickness cylindrical defect	Entire height of ossification centre	Mid-way	Proximal and distal	Medial and lateral	TIII	Adjacent ossification impinges	Medial defect is opposite medial defect in CTB
<i>u</i>	2	1x large, medium-depth, circumferential ovoid defect	Proximal margin of TIII ossification centre	Peripheral	Dorsomedial	Medial	TIII	Kissing repair in CTB	Suspect primary lesion because large defect
<i>v</i>	2	1x large vessel and protruding ossification tube repair response	Distal margin of CTB ossification centre	Peripheral	Dorsomedial	Medial	CTB	Not applicable	Suspect secondary repair because protrusion; near dorsal tarsal ligament
<i>w</i>	22 <sup>a</sup>	1x large, deep linear, shelf-like circumferential defect	Mid-height of dorsal aspect of TIII ossification centre	Peripheral	Dorsolateral	Lateral	TIII	Adjacent ossification impinges	Closely adjacent to distal surface defect
<i>x</i>	22 <sup>a</sup>	1x large, deep linear, groove-like circumferential defect	Distal aspect of TIII ossification centre	Mid-way	Dorsolateral	Lateral	TIII	None	Also small, circular defect distal ossification front, centrally near margin towards ligament fossa

Abbreviations: CTB, Central tarsal bone; TIII, Third tarsal bone.

<sup>a</sup>Additional suspect areas not listed due to small size, animal prevalence unaffected.

contained small, mineralised foci (Figure S3C). The TIII of foal 15 contained a small ossification centre with the three focal defects of osteochondrosis lesion *q15*, above (Figure S3E). The generalised changes in foals 3 and 15 were potentially compatible with incomplete ossification.

## 4 | DISCUSSION

With the current method, radiological osteochondrosis lesions were detected in 61% of the population, and perfusion yielded only partial information in 41% of the animals.

### 4.1 | Perfusion quality

The most important reasons why the perfusions were partial were probably that it was not possible to heparinise the animals ante-mortem,<sup>4</sup> the time from death to perfusion could not be controlled and most of the animals were sick, including conditions that affect circulation. Perfused vessels could be described, but when contrast columns were not visible, it was not possible to tell if this was due to vascular failure or perfusion failure. The barium used in the current study was expensive, the procedure was time-consuming and, in view of the partial results, we concluded that post-mortem perfusion is not recommended for future studies of the blood supply to the growth cartilage of the CTB and TIII. New techniques have been developed that do not require contrast perfusion, in particular susceptibility-weighted magnetic resonance imaging,<sup>24-26</sup> sensitive to haemoglobin in vessels, may be suitable for examination of small tarsal bones from post-mortem specimens. Once vessels regress, dimples disappear from the ossification front,<sup>17</sup> so the current results indicate that future studies of the blood supply to growth cartilage should focus on the CTB and TIII of foals  $\leq 105$  days old.

### 4.2 | Interpretation of focal defects as osteochondrosis lesions

The current interpretation of focal defects in the ossification front in micro-CT scans as osteochondrosis lesions was based on the fact that this has been histologically confirmed multiple times,<sup>17,18</sup> in multiple species, bones and sites,<sup>17,18,27</sup> including another cuboidal bone: the talus.<sup>17</sup> When Watrous et al<sup>11</sup> examined focal irregularities identified in radiographs of tarsal bone slabs histologically, they confirmed that the foci contained retained, hypertrophic cartilage or degenerated, necrotic cartilage. Vascular failure tends to result in ischaemic chondronecrosis in regions with poor collateral diffusion like epiphyseal growth cartilage,<sup>5,28</sup> and retention of viable, hypertrophic chondrocytes in regions with good collateral diffusion, like the metaphyseal growth plate.<sup>29</sup> The histological results of Watrous et al<sup>11</sup> therefore agree with osteochondrosis being due to vascular failure, and strengthen the argument based on published

literature,<sup>2,3,17,18</sup> that focal defects in the CTB and TIII ossification front should be interpreted as osteochondrosis lesions.

All current observed defects were focal or multi-focal. Endochondral ossification advances on growth cartilage that has three anatomical components: chondrocytes, extracellular matrix and blood supply.<sup>3,4</sup> The blood supply is the only component that is regularly spaced<sup>30</sup> and heterogeneously distributed<sup>4</sup> in a way that matches and can explain multi-focal lesions.<sup>18</sup> This supports the more specific argument that the current observed defects should be interpreted as osteochondrosis lesions due to vascular failure, simply by virtue of the fact that they were focal.<sup>18</sup> It is a limitation of the current study that the observed lesions were not histologically validated. The examined bones are currently being prepared for histology, and will be included in a future study.

### 4.3 | Pathogenesis of vascular failure in the CTB and TIII in context of the existing literature

In addition to the historical arguments, the current results contain some new evidence which suggests that a relationship exists between vessel configuration and lesion geometry in the CTB and TIII, as previously confirmed for osteochondrosis in other bones.<sup>4,18,31</sup> Proximodistally aligned lesions matched the configuration of vertical vessels, cylindrical lesions matched transverse vessels and lesions with circumferential long axes matched circumferential vessels. Two features of the blood supply were particularly noted because they have been implicated in the pathogenesis of vascular failure: incorporation of the mid-portion of vessels into bone, while the proximal and distal portions remained in growth cartilage,<sup>4,31</sup> and vessels entering growth cartilage at sites where ligaments also insert.<sup>32</sup> In both pigs<sup>31</sup> and foals,<sup>4</sup> early osteochondrosis lesions were consistently located around the portion of vessels immediately distal to incorporation into bone, suggesting that vessels were unable to withstand microscopic, biomechanical forces acting at the point where they traversed the junction between bone and growth cartilage, after incorporation.<sup>4,31</sup> In the current study, 12 lesions *a2-l22*, and parts of the three lesions *p11-r6* were located in regions where vessels emerged from the ossification front after incorporation. We therefore hypothesise that lesions located in regions of the CTB and TIII where vessels emerge from the ossification front after incorporation into bone may be the result of vascular failure during incorporation (Figure 6A-E).

Three lesions *m22-o12*, parts of the three lesions *p11-r6* and the two full-thickness lesions *s16-t16* were not located in any region where vessels emerged from bone after incorporation. When porcine early femoral lesions were followed back to the point of vascular failure using 3D, second harmonics generation microscopy, 11/14 failed vessels coursed to the ossification front, but the remaining 3/14 failed vessels did not course via bone and could not have failed during incorporation.<sup>32</sup> Instead, all 3/14 failed vessels entered growth cartilage at the site where the cranial cruciate ligament inserted.<sup>32</sup> Vascular failure may therefore sometimes occur because vessels are unable to withstand biomechanical forces acting at the point where they traverse

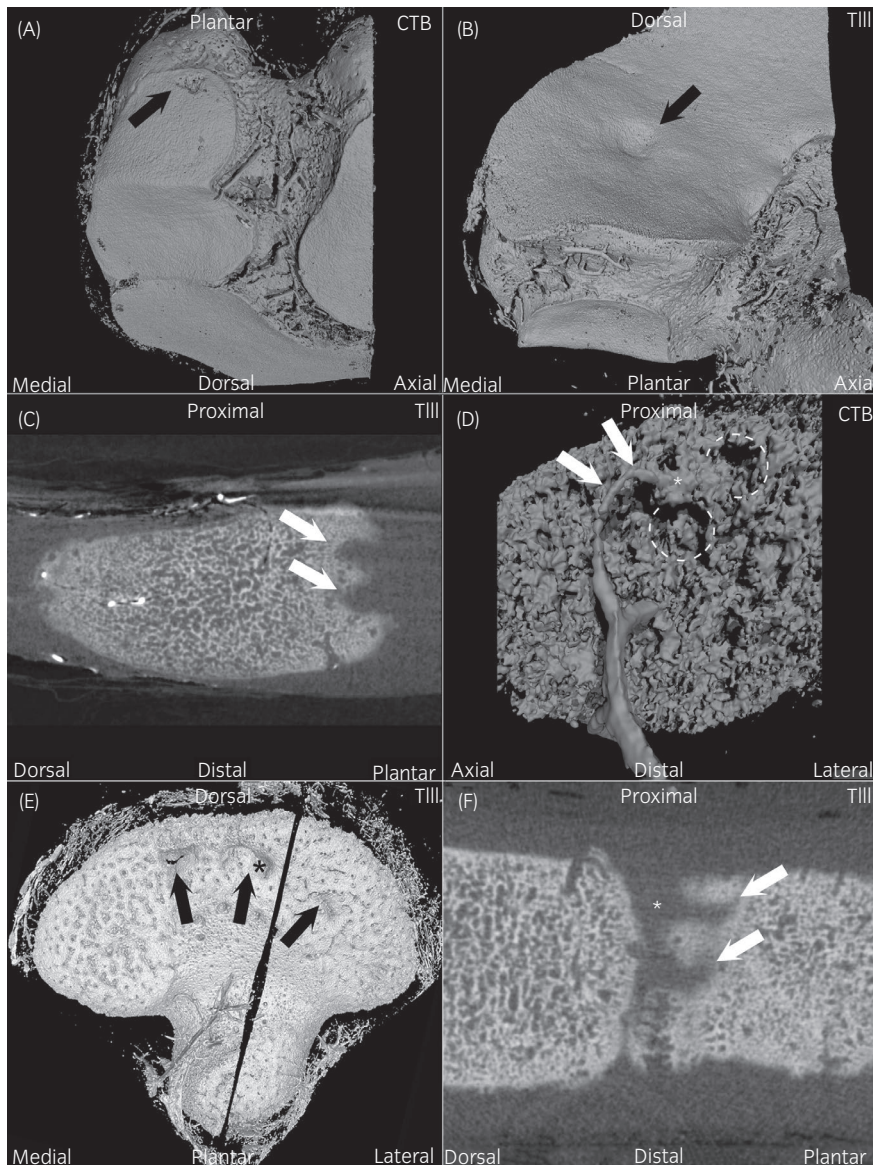


**FIGURE 4** Peripheral vertical lesions and axial transverse lesions, including side defects. A, The figure shows lesion *f23* (arrow), located in a region of the central tarsal bone (CTB) where vertical vessels emerge from the ossification front after incorporation of the mid-portion into bone (Figure 3D). Lesion *f23* is shallow and near the periphery, interpreted as short duration. B, The figure shows lesion *l22* (arrow), also located in a region where vessels emerge from the ossification front after incorporation, but it is deeper and near the centre of the third tarsal bone (TIII), interpreted as longer duration than lesion *f23* in A. Lesion *l22* is compatible with a cyst. C, Lesion *q15* is located at mid-height of TIII and includes two defect lobes (arrows) aligned in the proximo-distal direction, matching the configuration of side branches of vertical vessels (Figure 3D). D, Lesion *r6* is located at mid-height and near the proximal ossification front of the CTB, and includes two lobes (dashed circles) that are roughly aligned in the proximo-distal direction. Superficially adjacent, there is an intact, vertical vessel (arrows) where one side branch is surrounded by a mineral density (asterisk), interpreted as a separate centre of reparative ossification. E, Lesion *t16* consists of three vertical, full-thickness, cylindrical defects (arrows), matching the configuration of transverse vessels (Figure 3E). F, The middle cylinder in lesion *t16* (asterisks in E and F) has small side defects (arrows), matching side branches of transverse vessels (Figure 3E). A, Plantar and slightly distal view, B, Plantar and slightly proximal view, D, Plantar view, E, Proximal view of 3D bone and barium isosurface models; C, F, Sagittal slices

the junction between perichondrium and growth cartilage at sites where ligaments also insert.<sup>32</sup> Nutrient arteries entered the CTB and TIII via the inter-tarsal ligament fossae, and some perichondrial vessels entered growth cartilage where the dorsal tarsal ligament inserted. We therefore propose a second working hypothesis that lesions located distant from vessel incorporation into bone may be the result of

vascular failure at ligament insertion sites (Figure 6F-I). In the current study, four lesions *u2-x22* were compatible with failure of circumferential vessels (Figure 6J-N). Although, it was not explicitly observed, due to expansion of the ossification centre, circumferential vessels are likely to become incorporated into bone. Circumferential vessels may also enter growth cartilage at sites where collateral ligaments insert,

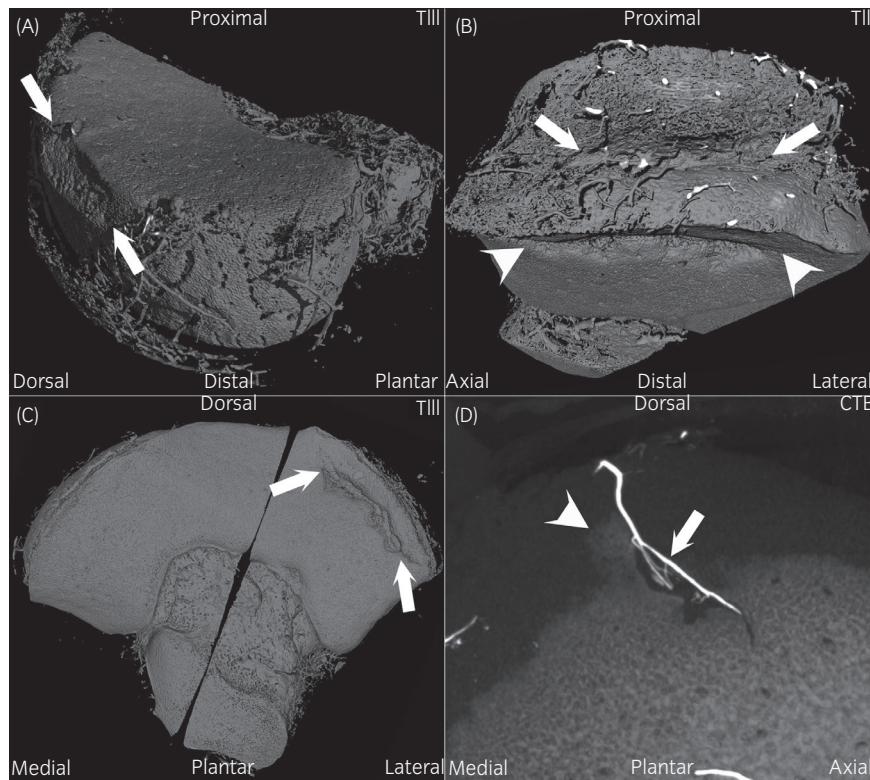


**FIGURE 5** Circumferential lesions. A, Lesion *u2* consists of an ovoid defect (between arrows) where the long axis of the ovoid is parallel with the circumference of the third tarsal bone (TIII), and parallel with circumferential vessels (Figure 3F). Lesion *u2* is shallow and peripheral, interpreted as short duration. B, Lesion *w22* consists of a circumferential, shelf-like defect (between arrows) at mid-height of the dorsolateral ossification front of the same TIII as lesion *x22*, just visible (between arrowheads). C, Lesion *x22* consists of a linear groove defect (between arrows) in the distal ossification front of TIII. Lesion *x22* is deeper and located near the centre, interpreted as longer duration than lesion *u2* in A. D, The change referred to as lesion *v2* consists of a large vessel (arrow), surrounded by a bony tube (arrowhead) protruding from the distal ossification front of the central tarsal bone (CTB) directly opposite and interpreted as a repair response to lesion *u2* in A. A, Dorsomedial view, B, Dorsolateral view and C, Distal view of 3D bone and barium isosurface models; D, Transverse slice

and to investigate the second working hypothesis, description of all ligament insertion sites on the CTB and TIII during the age range when cartilage canal vessels are present will be necessary.

#### 4.4 | Pathogenesis of multiple lesions

Lesion pairs *i20-j20*, *k22-l22* and *u2-v2* (Figure 5A,C) were located directly opposite to each other in the CTB and TIII. Lesions *i20-j20* and *k22-l22* were located the same distance from the periphery and therefore likely to have been initiated at the same time.<sup>5</sup> The dorsal tarsal ligament inserts on both the CTB and TIII, and could cause vessel failure in both bones simultaneously. Alternatively, the distal intermediate ridge of the tibia impinges on the small tarsal bones during maximal flexion, and could therefore cause vessel failure at the same time in the CTB and TIII.<sup>21</sup>

Lesion *v2* distally in the CTB was interpreted as a reparative response to lesion *u2* proximally in TIII (Figure 5A,C). Reparative responses<sup>4,5,17</sup> have only been reported in the bone with the osteochondrosis lesion, not in adjacent bones, but previously studied bone pairs: the tibia and talus,<sup>4,17</sup> third metatarsal bone and proximal phalanx,<sup>16</sup> are located further apart than the small tarsal bones. For

a short time after vascular failure, chondrocytes stain immunopositive for vascular endothelial growth factor,<sup>33</sup> and it is at least theoretically possible that the CTB and TIII are so closely apposed that vessels in one bone may respond to signals from lesions in the other one.

Even with the two proposed working hypotheses (Figure 6), it is difficult to see how defects could be initiated in five sites simultaneously in foal 16 (Figure 4E). However, foal 16 was culture-positive for *Escherichia coli*, and it was recently confirmed that bacteria can occlude blood supply and trigger the same pathogenesis as heritably predisposed, aseptic vascular failure in foals.<sup>34</sup> The mechanism is that cartilage canal vessels have discontinuities<sup>35</sup> that enable circulating bacteria to come into contact with matrix components they have a binding affinity for,<sup>36</sup> leading to vessel occlusion.<sup>37</sup> Initially, bacteria can bind anywhere discontinuities are present when they enter the circulation, either constitutionally or as part of normal development, for example: vessel in-growth<sup>37</sup> and regression.<sup>35</sup> Subsequently, more discontinuities also open up under the influence of bacteria and neutrophils,<sup>38</sup> enabling further binding. When there are multiple discontinuities, circulating bacteria can bind and cause vascular occlusion in multiple sites. Bacteria may have been eliminated, but sections from

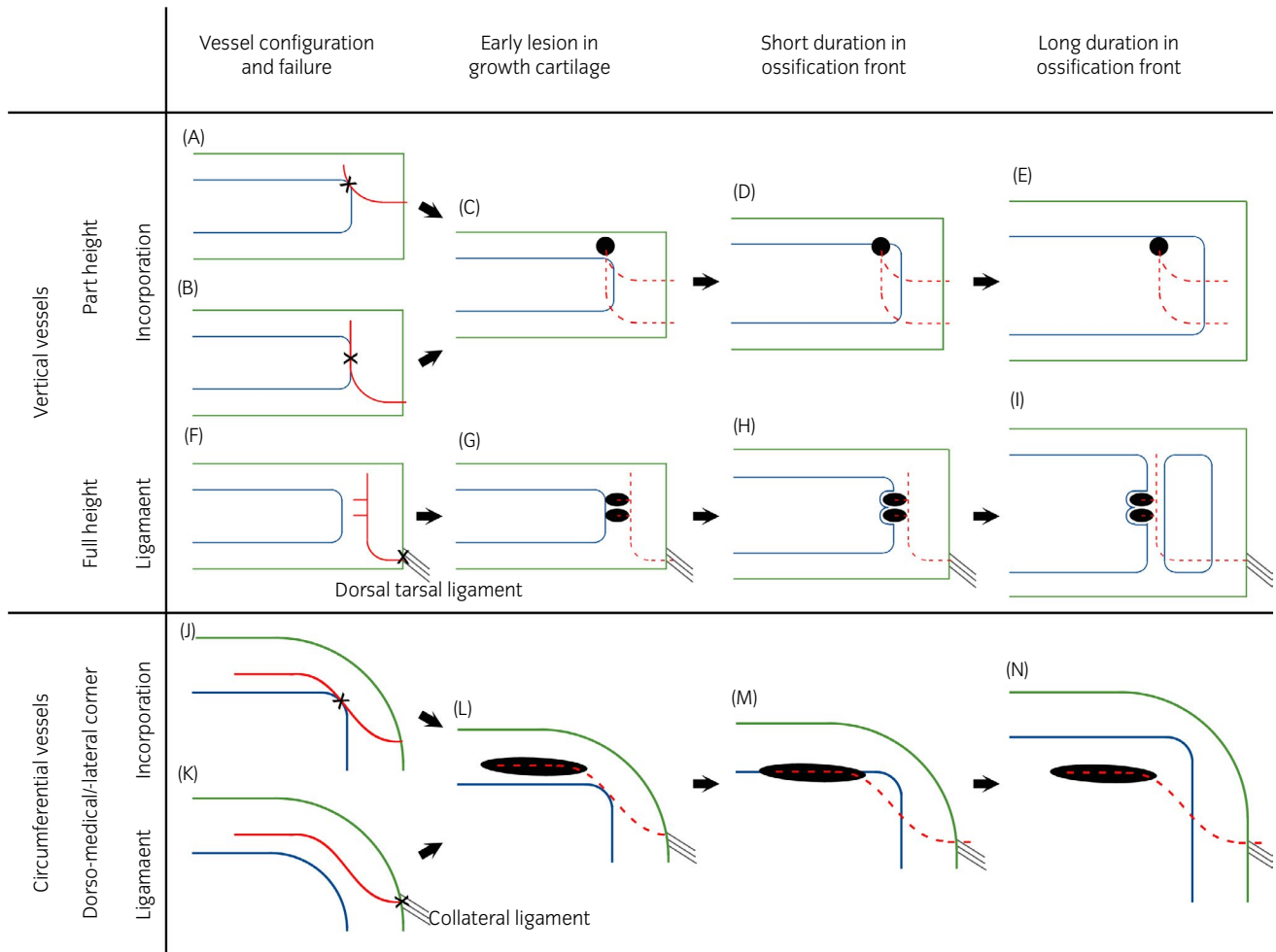


**FIGURE 6** Diagram of hypotheses relating failure of vessels to the pathogenesis of osteochondrosis lesions in the distal tarsus. A-E, Failure of vertical vessels during incorporation into bone. Vessels course vertically for A, part, or B, full height of the ossification centre. The mid-portion of vertical vessels is incorporated into bone, while the proximal and distal portions remain in growth cartilage. Vascular failure (x) occurs, and results in C, early lesions (black circle) at intermediate depth of growth cartilage, outside diffusion distance from collateral supply. Endochondral ossification progresses adjacent to the lesion, which after D, short duration, constitutes a shallow defect near the periphery of the ossification centre, and after E, long duration, constitutes a deeper defect near the axial centre of the bone. F-I, Failure of vertical vessels at ligament insertion sites, including side branches. Vertical vessels with side branches enter growth cartilage where F, the dorsal tarsal ligament inserts, and failure occurs (x). This results in early lesions (black circles) around trunks and branches in growth cartilage outside diffusion distance from collateral supply. Endochondral ossification progresses adjacent to lesions, which after H, short duration, constitute multi-lobulated defects in the ossification front, and after I, long duration, constitute transverse, cylindrical lesions with side defects near the axial centre of the bone. J-N, Failure of circumferential vessels. J-K, Vessels course horizontally and parallel with the circumference of the bone. Either J, the mid-portion of vessels is incorporated into bone, or K, vessels enter growth cartilage where the collateral ligament inserts, and failure occurs (x). This results in L, an early lesion (black circle) in growth cartilage outside diffusion distance from collateral supply. Endochondral ossification progresses adjacent to the lesion, which after M, short duration, constitutes a shallow defect near the periphery of the ossification centre, and after E, long duration, constitutes a deeper defect near the axial centre of the bone. A-I, Sagittal slices. J-N, Transverse slices

foal 16 will nevertheless be scrutinised for bacteria and neutrophils<sup>34</sup> during the up-coming histological validation.

#### 4.5 | The importance of the sinusoids

The geometry of the cylindrical defects in foal 16 was a perfect match for failure and delayed endochondral ossification around vertical cartilage canal vessels. One might consider that osteomyelitis

is an appropriate differential diagnosis for the defects in foal 16. However, osteomyelitis entails necrosis and destruction of already formed bone, and it is difficult to see why such bone loss should be confined to cylinders matching the blood supply to growth cartilage. The suspected pathogenesis of vascular failure in foal 16 may still be important to osteomyelitis. The current observed small-to-medium sinusoids appeared to represent anatomical structures. Extra-large sinusoids were more compatible with vessel rupture and barium leakage into marrow spaces, but such leakage need not

represent technical error; it could be genuine, due to vessels being disposed to rupture in sick foals.<sup>38</sup> Firth and Goedegebuure<sup>39</sup> concluded that the infection in osteomyelitis starts in sinusoids in subchondral bone, but it is still poorly understood why it should start more frequently in some regions of some bones, than others. It is important to determine if sinusoidal vessels in subchondral bone are discontinuous and enable bacterial binding by a similar mechanism to the bacterial binding in growth cartilage canals suspected in foal 16.<sup>34,37</sup> If so, mapping of sinusoids could explain why osteomyelitis starts more frequently in some regions than others,<sup>39</sup> and improve our understanding of the progression and outcome of this serious condition.

#### 4.6 | Was there any new evidence of whether osteochondrosis causes distal tarsal osteoarthritis?

Osteochondrosis can resolve or persist,<sup>6,7</sup> and the current lesions included reparative responses<sup>17</sup> that could enable lesions to undergo spontaneous resolution. In this context, it was noted that the CTB and TIII increased three times as much in the lateromedial and dorso-plantar dimensions, as in proximodistal height. This translates to lesions located in the abaxial ossification front being three times more likely to become completely surrounded by bone and resolve,<sup>17</sup> than lesions in the proximal and distal ossification fronts, which are more likely to persist.

The prevalence of early osteochondrosis was 75% in the Icelandic group, comparable to the 72% prevalence reported by Watrous et al.<sup>11</sup> A proportion of osteochondrosis lesions will resolve before screening age,<sup>6,7,40</sup> and heritably predisposed<sup>12</sup> Icelandic Horses radiographed for distal tarsal osteoarthritis from 5 years old have a prevalence of 30% at mean age 7.9 years.<sup>13</sup> Some of the current observed changes overlap with changes detected when young Icelandic<sup>41-44</sup> and other horses<sup>11,14,22</sup> are examined for early, distal tarsal osteoarthritis. Osteochondrosis defects potentially overlap with defects observed in early osteoarthritis.<sup>11,14,41,43,44</sup> In particular, the groove defect in lesion x22 (Figure 5C) appears to overlap with the 'arrest trenches' seen in 30-month-old Icelandic Horses.<sup>43</sup> It has been suggested that marginal osteophytes in osteoarthritis do not genuinely protrude, but rather appear to protrude because there is a defect axially adjacent to them,<sup>11,14,41,43,44</sup> in which case this would also fit with continued endochondral ossification around and abaxial to the defect in lesion x22 (Figure 5B,C). The reparative ossification tube in lesion v2 (Figure 5D) was potentially likely to persist because it protruded from the distal ossification front of the CTB where there was less growth, and could overlap with focal, marginal osteophytes in osteoarthritis.<sup>11,14,42-44</sup> Whether osteochondrosis causes distal tarsal osteoarthritis can only be determined by monitoring lesions longitudinally, and, pending the outcome of histological validation, the current micro-CT diagnoses can be translated to conventional CT and used to follow lesions over time, as previously done in pigs.<sup>40</sup>

#### 4.7 | Other lesions

The coarse patches in the ossification front of foal 1 did not readily match any developmental disease,<sup>1</sup> but it could just be that they represent an early, unfamiliar stage of an otherwise well-known disease. The bones of foal 3 were poorly ossified, but it was born 6 weeks prematurely and ossification may have been appropriate for the given gestation length.<sup>9,45</sup> Foal 15 was normal weight for the breed, and although it had contracted forelimb tendons and incompletely ossified carpal bones, it did not have any other signs of prematurity and was assumed to have normal gestation length. Foal 15 had the three osteochondrosis defects of lesion q15 in the small ossification centre of TIII (Figure 4C; Figure S3E), indicative of focal vascular disease.<sup>3,5,17</sup> Cartilage canal vessels are present before, and essential to formation of both primary and secondary ossification centres.<sup>46</sup> Incomplete ossification can therefore plausibly be a result of earlier, more generalised vascular disease. We will attempt to clarify the nature of the changes in foals 1, 3 and 15 during histological validation.

## 5 | CONCLUSIONS

Post-mortem perfusion was poor for examination of the blood supply to the growth cartilage of the CTB and TIII. Radiological osteochondrosis lesions were compatible with vascular failure because they were focal, and because lesion geometry matched vessel configuration. The relationship between osteochondrosis and distal tarsal osteoarthritis warrants further investigation, including validation of the current lesions and longitudinal monitoring.

#### ACKNOWLEDGEMENTS

The authors are grateful to Doctor Liebert P. Nogueira at the University of Oslo for performing the micro-CT scans. The authors would like to thank Professors Kerstin Hansson and Stina Ekman at the Swedish University of Agricultural Sciences for helpful discussions during the project.

#### ETHICAL ANIMAL RESEARCH

The study was approved by the institutional ethics committee (project number H-16-47-192).

#### INFORMED CONSENT

Owners gave consent for their animals' inclusion in the study.

#### CONFLICT OF INTERESTS

No competing interests have been declared.

#### AUTHORSHIP

All authors contributed to study design, data acquisition and interpretation. S. Sigurdsson, K. Olstad and C.T. Fjordbakk had full access

to all data. S. Sigurdsson and K. Olstad drafted the manuscript and all authors critically revised and approved the final version. K. Olstad is the responsible author.

## PEER REVIEW

The peer review history for this article is available at <https://publons.com/publon/10.1111/evj.13432>.

## DATA ACCESSIBILITY STATEMENT

The data that support the findings of this study are available on request from the corresponding author. The data are not publicly available due to privacy or ethical restrictions.

## ORCID

Kristin Olstad  <https://orcid.org/0000-0001-6770-3403>

Sigríður Björnsdóttir  <https://orcid.org/0000-0001-5521-475X>

## REFERENCES

- Ed: C.W. McIlwraith Developmental Orthopedic Disease Symposium. Dallas-Forth Worth: The American Quarter Horse Association, 1986; pp 1–77.
- Rejnö S, Strömberg B. Osteochondrosis in the horse. II. pathology. *Acta radiologica. Supplementum*. 1978;358:153–78.
- Carlson CS, Cullins LD, Meuten DJ. Osteochondrosis of the articular-epiphyseal cartilage complex in young horses: evidence for a defect in cartilage canal blood supply. *Vet Pathol*. 1995;32(6):641–7.
- Olstad K, Ytrehus B, Ekman S, Carlson CS, Dolvik NI. Epiphyseal cartilage canal blood supply to the tarsus of foals and relationship to osteochondrosis. *Equine Vet J*. 2008;40(1):30–9.
- Olstad K, Hendrickson EHS, Carlson CS, Ekman S, Dolvik NI. Transection of vessels in epiphyseal cartilage canals leads to osteochondrosis and osteochondrosis dissecans in the femoro-patellar joint of foals; a potential model of juvenile osteochondritis dissecans. *Osteoarthritis Cartilage*. 2013;21:730–8.
- Carlsten J, Sandgren B, Dalin G. Development of osteochondrosis in the tarsocrural joint and osteochondral fragments in the fetlock joints of Standardbred trotters. I. A radiological survey. *Equine Vet J*. 1993;25(Suppl 16):42–7.
- Dik KJ, Enzerink E, van Weeren PR. Radiographic development of osteochondral abnormalities in the hock and stifle of Dutch Warmblood foals, from age 1 to 11 months. *Equine Vet J*. 1999;31(Suppl 31):9–15.
- Olstad K, Ostevik L, Carlson CS, Ekman S. Osteochondrosis can lead to formation of pseudocysts and true cysts in the subchondral bone of horses. *Vet Pathol*. 2015;52(5):862–72.
- Coleman MC, Whitfield-Cargile C. Orthopedic conditions of the premature and dysmature foal. *Veterinary Clin North America. Equine Practice*. 2017;33(2):289–97.
- Sprackman L, Dakin SG, May SA, Weller R. Relationship between the shape of the central and third tarsal bones and the presence of tarsal osteoarthritis. *Vet J*. 2015;204(1):94–8.
- Watrous BJ, Hultgren BD, Wagner PC. Osteochondrosis and juvenile spavin in equids. *Am J Vet Res*. 1991;52(4):607–12.
- Arnason T, Björnsdóttir S. Heritability of age-at-onset of bone spavin in Icelandic horses estimated by survival analysis. *Livest Prod Sci*. 2003;79:285–93.
- Björnsdóttir S, Axelsson M, Eksell P, Sigurdsson H, Carlsten J. Radiographic and clinical survey of degenerative joint disease in the distal tarsal joints in Icelandic horses. *Equine Vet J*. 2000;32(3):268–72.
- Lavery S, Stover SM, Belanger D, O'Brien TR, Pool RR, Pascoe JR, et al. Radiographic, high detail radiographic, microangiographic and histological findings of the distal portion of the tarsus in weanling, young and adult horses. *Equine Vet J*. 1991;23(6):413–21.
- Olstad K, Ytrehus B, Ekman S, Carlson CS, Dolvik NI. Epiphyseal cartilage canal blood supply to the distal femur of foals. *Equine Vet J*. 2008;40(5):433–9.
- Olstad K, Ytrehus B, Ekman S, Carlson CS, Dolvik NI. Epiphyseal cartilage canal blood supply to the metatarso-phalangeal joint of foals. *Equine Vet J*. 2009;41(9):865–71.
- Olstad K, Cnudde V, Masschaele B, Thomassen R, Dolvik NI. Micro-computed tomography of early lesions of osteochondrosis in the tarsus of foals. *Bone*. 2008;43(3):574–83.
- Olstad K, Kongsro J, Grindflek E, Dolvik NI. Ossification defects detected in CT scans represent early osteochondrosis in the distal femur of piglets. *J Orthop Res*. 2014;32(8):1014–23.
- Firth EC, Poulos PW. Blood vessels in the developing growth plate of the equine distal radius and metacarpus. *Res Vet Sci*. 1982;33(2):159–66.
- Firth EC, Poulos PW. Vascular characteristics of the cartilage and subchondral bone of the distal radial epiphysis of the young foal. *N Z Vet J*. 1993;41(2):73–7.
- Hertsch B, Samy MT. Arteriographic studies of the distal tibial end in relation to the pathogenesis of osteochondrosis dissecans in the horse. *Zentralbl Veterinarmed A*. 1980;27(6):469–78.
- Barneveld A, van Weeren PR. Early changes in the distal intertarsal joint of Dutch Warmblood foals and the influence of exercise on bone density in the third tarsal bone. *Equine Vet J*. 1999;31(Suppl 31):67–73.
- Wormstrand BH, Fjordbakk CT, Griffiths DJ, Lykkjen S, Olstad K. Development of the blood supply to the growth cartilage of the medial femoral condyle of foals. *Equine Vet J*. 2021;53(1):134–42.
- Toth F, Nissi MJ, Zhang J, Benson M, Schmitter S, Ellermann JM, et al. Histological confirmation and biological significance of cartilage canals demonstrated using high field MRI in swine at predilection sites of osteochondrosis. *J Orthop Res*. 2013;31(12):2006–12.
- Martel G, Kiss S, Gilbert G, Anne-Archard N, Richard H, Moser T, et al. Differences in the vascular tree of the femoral trochlear growth cartilage at osteochondrosis-susceptible sites in foals revealed by SWI 3T MRI. *J Orthop Res*. 2016;34(9):1539–46.
- Martel G, Forget C, Gilbert G, Richard H, Moser T, Olive J, et al. Validation of the ultrasonographic assessment of the femoral trochlea epiphyseal cartilage in foals at osteochondrosis predilected sites with magnetic resonance imaging and histology. *Equine Vet J*. 2017;49(6):821–8.
- Toth F, Nissi MJ, Wang L, Ellermann JM, Carlson CS. Surgical induction, histological evaluation, and MRI identification of cartilage necrosis in the distal femur in goats to model early lesions of osteochondrosis. *Osteoarthritis Cartilage*. 2014;23(2):300–7.
- Carlson CS, Meuten DJ, Richardson DC. Ischemic necrosis of cartilage in spontaneous and experimental lesions of osteochondrosis. *J Orthop Res*. 1991;9(3):317–29.
- Olstad K, Wormstrand B, Kongsro J, Grindflek E. Osteochondrosis in the distal femoral physis of pigs starts with vascular failure. *Vet Pathol*. 2019;56(5):732–42.
- Wilsman NJ, Van Sickle DC. Cartilage canals, their morphology and distribution. *Anat Rec*. 1972;173(1):79–93.
- Ytrehus B, Ekman S, Carlson CS, Teige J, Reinholt FP. Focal changes in blood supply during normal epiphyseal growth are central in the pathogenesis of osteochondrosis in pigs. *Bone*. 2004;35(6):1294–306.

32. Finnøy A, Olstad K, Lilledahl MB. Non-linear optical microscopy of cartilage canals in the distal femur of young pigs may reveal the cause of articular osteochondrosis. *BMC Vet Res.* 2017;13(1):270.
33. Hellings IR. Differences between cartilage canals with relevance for osteochondrosis in horses, PhD Thesis, Norwegian University of Life Sciences, Oslo, Norway; 2017.
34. Wormstrand B, Ostevik L, Ekman S, Olstad K. Septic Arthritis/osteomyelitis may lead to osteochondrosis-like lesions in foals. *Vet Pathol.* 2018;55(5):693–702.
35. Hellings IR, Ekman S, Hultenby K, Dolvik NI, Olstad K. Discontinuities in the endothelium of epiphyseal cartilage canals and relevance to joint disease in foals. *J Anat.* 2016;228(1):162–75.
36. Chagnot C, Listrat A, Astruc T, Desvaux M. Bacterial adhesion to animal tissues: protein determinants for recognition of extracellular matrix components. *Cell Microbiol.* 2012;14(11):1687–96.
37. Speers DJ, Nade SM. Ultrastructural studies of adherence of *Staphylococcus aureus* in experimental acute hematogenous osteomyelitis. *Infect Immun.* 1985;49(2):443–6.
38. Razakandrainibe R, Combes V, Grau GE, Jambou R. Crossing the wall: the opening of endothelial cell junctions during infectious diseases. *Int J Biochem Cell Biol.* 2013;45(7):1165–73.
39. Firth EC, Goedegebuure SA. The site of focal osteomyelitis lesions in foals. *Vet Q.* 1988;10(2):99–108.
40. Olstad K, Kongsro J, Grindflek E, Dolvik NI. Consequences of the natural course of articular osteochondrosis in pigs for the suitability of computed tomography as a screening tool. *BMC Vet Research.* 2014;10(1):212.
41. Björnsdóttir S, Ekman S, Eksell P, Lord P. High detail radiography and histology of the centrodistal tarsal joint of Icelandic horses age 6 months to 6 years. *Equine Vet J.* 2004;36(1):5–11.
42. Ley CJ, Ekman S, Dahlberg LE, Björnsdóttir S, Hansson K. Evaluation of osteochondral sample collection guided by computed tomography and magnetic resonance imaging for early detection of osteoarthritis in centrodistal joints of young Icelandic horses. *Am J Vet Res.* 2013;74(6):874–87.
43. Ley CJ, Ekman S, Hansson K, Björnsdóttir S, Boyde A. Osteochondral lesions in distal tarsal joints of Icelandic horses reveal strong associations between hyaline and calcified cartilage abnormalities. *Eur cell mater.* 2014;27:213–36.
44. Ley CJ, Björnsdóttir S, Ekman S, Boyde A, Hansson K. Detection of early osteoarthritis in the centrodistal joints of Icelandic horses: Evaluation of radiography and low-field magnetic resonance imaging. *Equine Vet J.* 2016;48(1):57–64.
45. Sedrish SA, Moore RM. Diagnosis and management of incomplete ossification of the cuboidal bones in foals. *Equine Practice.* 1997;19(5):16–21.
46. Blumer MJF, Longato S, Fritsch H. Structure, formation and role of cartilage canals in the developing bone. *Ann Anat.* 2008;190:305–15.

#### SUPPORTING INFORMATION

Additional supporting information may be found online in the Supporting Information section.

**How to cite this article:** Sigurdsson SF, Olstad K, Ley CJ, Björnsdóttir S, Griffiths DJ, Fjordbakk CT. Radiological, vascular osteochondrosis occurs in the distal tarsus, and may cause osteoarthritis. *Equine Vet J.* 2022;54:82–96. <https://doi.org/10.1111/evj.13432>

## A Practical Guide to Equine Radiography

Editors: Gabriel Manso-Díaz, Javier López-Sanromán and Renate Weller

Publisher: 5m Publishing, December 2018 • Hardback, 200 pages

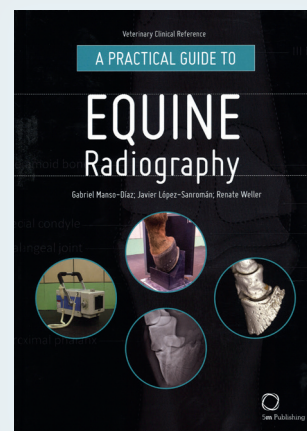
*A Practical Guide to Equine Radiography* is designed to accompany the clinical veterinarian either within a hospital setting or out in the field. The book offers an informative step-by-step guide to obtaining high quality radiographs with a focus on image quality, accuracy, consistency and safety. General principles and equipment are covered before working through the anatomy of the horse with separate chapters devoted to each body region, providing a thorough and detailed picture of the skeletal structure of the horse, making the book an ideal reference for equine practitioners, veterinary students and para-professionals.

The veterinarian is guided through the stages of taking and interpreting normal radiographs including: Clinical indications of radiographic areas of interest in the horse; Equipment required; Preparation and setup guides; Projections focusing on radiographic areas of interest; X-rays presented with detailed labels, providing a close-up view of skeletal structures; Three dimensional images demonstrating normal anatomy.

**Gabriel Manso-Díaz**, DVM, MSc, PhD, MRCVS, Diagnostic Imaging Department, Complutense University of Madrid, Spain, and Equine Diagnostic Imaging Department, Royal Veterinary College, London, UK.

**Javier López-Sanromán**, DVM, PhD, DiplECVS, Associate Professor, Department of Animal Medicine and Surgery, Complutense University of Madrid, Spain.

**Renate Weller**, Dvmetmed, PhD, MScVetEd, FHEA, NTF, DiplACVSMR, DiplECVSMR, AssocECVDI, MRCVS, Professor of Comparative Imaging and Biomechanics, Royal Veterinary College, London, UK.



BEVA Member: £52.65  
Non Member: £65.00

**BEVA** Bookshop



www.beva.org.uk • 01638 723555 • [bookshop@evj.co.uk](mailto:bookshop@evj.co.uk)